NASA/TM—2002-211478

Cyclic Failure Mechanisms of Thermal and Environmental Barrier Coating Systems Under Thermal Gradient Test Conditions

Dongming Zhu
Ohio Aerospace Institute, Brook Park, Ohio

Kang N. Lee
Cleveland State University, Cleveland, Ohio

Robert A. Miller
Glenn Research Center, Cleveland, Ohio

April 2002

The NASA STI Program Office . . . in Profile

Since its founding, NASA has been dedicated to the advancement of aeronautics and space science. The NASA Scientific and Technical Information (STI) Program Office plays a key part in helping NASA maintain this important role.

The NASA STI Program Office is operated by Langley Research Center, the Lead Center for NASA's scientific and technical information. The NASA STI Program Office provides access to the NASA STI Database, the largest collection of aeronautical and space science STI in the world. The Program Office is also NASA's institutional mechanism for disseminating the results of its research and development activities. These results are published by NASA in the NASA STI Report Series, which includes the following report types:

- TECHNICAL PUBLICATION. Reports of completed research or a major significant phase of research that present the results of NASA programs and include extensive data or theoretical analysis. Includes compilations of significant scientific and technical data and information deemed to be of continuing reference value. NASA's counterpart of peer-reviewed formal professional papers but has less stringent limitations on manuscript length and extent of graphic presentations.

- TECHNICAL MEMORANDUM. Scientific and technical findings that are preliminary or of specialized interest, e.g., quick release reports, working papers, and bibliographies that contain minimal annotation. Does not contain extensive analysis.

- CONTRACTOR REPORT. Scientific and technical findings by NASA-sponsored contractors and grantees.

- CONFERENCE PUBLICATION. Collected papers from scientific and technical conferences, symposia, seminars, or other meetings sponsored or cosponsored by NASA.

- SPECIAL PUBLICATION. Scientific, technical, or historical information from NASA programs, projects, and missions, often concerned with subjects having substantial public interest.

- TECHNICAL TRANSLATION. English-language translations of foreign scientific and technical material pertinent to NASA's mission.

Specialized services that complement the STI Program Office's diverse offerings include creating custom thesauri, building customized data bases, organizing and publishing research results . . . even providing videos.

For more information about the NASA STI Program Office, see the following:

- Access the NASA STI Program Home Page at ***http://www.sti.nasa.gov***

- E-mail your question via the Internet to help@sti.nasa.gov

- Fax your question to the NASA Access Help Desk at 301–621–0134

- Telephone the NASA Access Help Desk at 301–621–0390

- Write to:
  NASA Access Help Desk
  NASA Center for AeroSpace Information
  7121 Standard Drive
  Hanover, MD 21076

NASA/TM—2002-211478

Cyclic Failure Mechanisms of Thermal and Environmental Barrier Coating Systems Under Thermal Gradient Test Conditions

Dongming Zhu
Ohio Aerospace Institute, Brook Park, Ohio

Kang N. Lee
Cleveland State University, Cleveland, Ohio

Robert A. Miller
Glenn Research Center, Cleveland, Ohio

Prepared for the
26th Annual International Conference on Advanced Ceramics and Composites
sponsored by the American Ceramics Society
Cocoa Beach, Florida, January 13–18, 2002

National Aeronautics and
Space Administration

Glenn Research Center

April 2002

Acknowledgments

This work was supported by NASA Ultra-Efficient Engine Technology (UEET) Program. The authors are grateful to George W. Leissler, QSS Group, Inc. at NASA Glenn Research Center, for his assistance in the preparation of plasma-sprayed TBC/EBC coatings.

Cyclic Failure Mechanisms of Thermal and Environmental Barrier Coating Systems Under Thermal Gradient Test Conditions

Dongming Zhu
Ohio Aerospace Institute
Brook Park, Ohio 44142

Kang N. Lee
Cleveland State University
Cleveland, Ohio 44115

Robert A. Miller
National Aeronautics and Space Administration
Glenn Research Center
Cleveland, Ohio 44135

ABSTRACT

Plasma-sprayed ZrO_2–8wt%Y_2O_3 and mullite+BSAS/Si multilayer thermal and environmental barrier coating (TBC-EBC) systems on SiC/SiC ceramic matrix composite (CMC) substrates were thermally cyclic tested under high thermal gradients using a laser high-heat-flux rig in conjunction with furnace exposure in water-vapor environments. Coating sintering and interface damage were assessed by monitoring the real-time thermal conductivity changes during the laser heat-flux tests and by examining the microstructural changes after exposure. Sintering kinetics of the coating systems were also independently characterized using a dilatometer. It was found that the coating failure involved both the time-temperature dependent sintering and the cycle frequency dependent cyclic fatigue processes. The water vapor environments not only facilitated the initial coating conductivity increases due to enhanced sintering and interface reaction, but also promoted later conductivity reductions due to the accelerated coating cracking and delamination. The failure mechanisms of the coating systems are also discussed based on the cyclic test results and are correlated to the sintering and thermal stress behavior under the thermal gradient test conditions.

INTRODUCTION

Environmental barrier coatings (EBCs) have been developed to protect SiC-based ceramic components in gas turbine engines from high temperature environmental attack [1-3]. With continuously increasing demands for significantly higher engine operating temperature, future EBC systems must be designed for both thermal and environmental protection of the engine components in gas turbine combustion environments [4]. The thermal barrier function of the coating systems will provide the necessary temperature reductions, thus lowering the engine component thermal loads and chemical reaction rates. Operation at reduced temperatures will better maintain the mechanical properties and extend the durability of these components.

In order to develop high performance ceramic coating systems, advanced high heat flux testing approaches were established [5-11]. The high heat flux tests based on a high power CO_2 laser approach made possible heating of the coating surface to significantly higher temperatures (e.g., 1500°C to 1650°C), while establishing a large thermal gradient across the coating thickness through the laser surface heating and backside air cooling. The coating operating temperature and stress conditions were more realistically simulated during test exposure.

Besides the advantages of realistic thermal gradient testing of the coating specimens at very high surface temperatures required in future engines, the coating thermal conductivity and sintering properties can also be obtained in real-time from the high heat flux tests. In addition, coating delaminations can be monitored as a function of cycle numbers from the observed thermal conductivity variations because coating delamination cracking causes an apparent decrease in the measured thermal conductivity. The laser approach has demonstrated certain advantages in evaluating environmental barrier coatings on SiC/SiC substrates because the unusual conductivity changes can be detected *in-situ* during the thermal cycling. As an example (shown in Fig. 1 (a)), a significant coating conductivity increase was observed during a laser thermal cyclic testing of a barium-strontium-aluminosilicate (BSAS) coating system [12], due to the formation of a surface glass phase and an interface high Si phase in the BSAS coating.

In this study, the laser high heat-flux based technique has been employed to investigate thermal cyclic behavior of a multi-layered ZrO_2–$8Y_2O_3$ thermal barrier and mullite+BSAS mixture/Si environmental barrier coating on SiC/SiC ceramic matrix composite substrates. In some cases, the laser thermal gradient tests in ambient air were combined with the furnace thermal cyclic tests in water-vapor environments for testing the coating specimens. The alternating laser test in conjunction with the furnace thermal cyclic test can provide the information about the water vapor effect on coating failure. The coating thermal conductivity, sintering, cracking and delamination were evaluated during these thermal cycling tests. The coating failure mechanisms are discussed based on the cyclic test results and correlated to the sintering, creep, and thermal stress behavior under the test temperature and heat flux conditions.

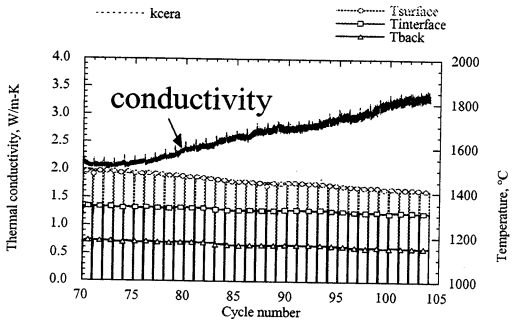

(a)

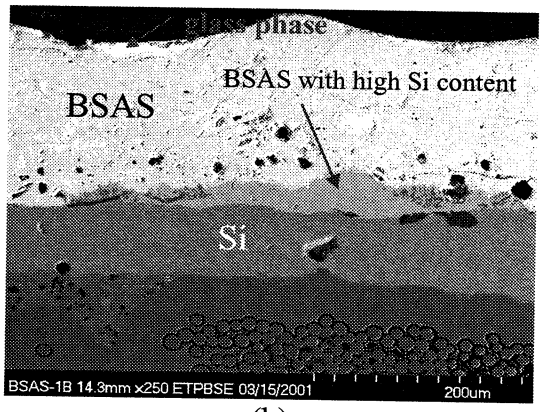

(b)

Fig. 1 A significant coating thermal conductivity rise was detected when the BSAS coating reacts with the Si layer, forming appreciable amount of high Si content phases at the interface. The surface glass phase was also observed during the laser thermal cyclic test at 1482°C (1 hr cycles) that may also contributes to the observed conductivity increase. (a) Thermal conductivity change during the laser cyclic test; (b) Coating cross-section micrograph of the BSAS coating.

EXPERIMENTAL MATERIALS AND METHODS

Materials

Plasma-sprayed ZrO_2–8wt%Y_2O_3 thermal barrier and mullite+BSAS/Si environmental barrier coatings on SiC/SiC ceramic matrix composites were investigated in this study. The EBC systems, namely, mullite and BSAS mixture layer and Si bond coat, were air plasma-sprayed (APS) onto 25.4 mm-diameter and 2.2 mm-thick melt infiltrated (MI) SiC/SiC ceramic composite substrates on a hot stage of a furnace. Substrate heating ensured deposition of the desired crystalline phases of these coating materials. The top ZrO_2–8wt%Y_2O_3 coating was then deposited using a conventional APS technique. The nominal thicknesses of the ZrO_2–8wt%Y_2O_3 top coat, mullite+BSAS mixture coat and Si layer were 254 μm, 330 μm, and 127 μm, respectively.

Thermal Cycling Tests

Thermal gradient cyclic testing of the ceramic coating materials was conducted using a 3.0 kW CO_2 laser (wavelength 10.6 μm) high-heat flux rig. The general test approaches have been described elsewhere [7, 9, 12-14]. In this laser heat flux test, the coating specimen surface heating was provided by the laser beam, and backside air cooling was used to maintain the desired specimen temperatures. A uniform laser heat flux was obtained over the 23.9 mm diameter aperture region of the specimen surface by using an integrating ZnSe lens combined with the specimen rotation. Platinum wire flat coils (wire diameter 0.38 mm) were used to form thin air gaps between the top platinum-coated stainless-steel plate and bottom stainless-steel back plate to minimize the specimen heat losses through the fixture. During the laser thermal cycling test, the ceramic surface temperature was measured by an 8 μm infrared pyrometer, and the backside CMC surface was measured by a two-color pyrometer. The real-time thermal conductivity of the coating system can also be obtained by measuring the temperature difference across the coating system.

The TBC/EBC coatings were thermally cycled in ambient air under the laser imposed thermal gradients. The surface was tested at approximately 1482°C, and the interface temperature was at either 1250°C or 1300°C. Thermal conductivity of the ceramic coating system was also monitored as a function of the laser cycle number using the steady-state laser heat flux test approach described above [7, 9, 10, 12-15]. Some coatings specimens were also subject to alternating the laser thermal gradient cycling tests in air and the furnace thermal cycling tests in a 90%H_2O-balance O_2 environment at 1300°C to investigate the water vapor effect. The laser thermal cyclic tests were conducted using either 30 or 60 min hot time temperature cycles, but all with 3 min cooling between each cycle to ensure that the test specimens were cooled below 100°C. Furnace cyclic tests consisted of 60 min high temperature heating and 20 min cooling cycles.

Sintering Behavior of the Coatings Materials

The sintering behavior of freestanding plasma-sprayed ZrO_2–8wt%Y_2O_3 and mullite coatings was determined using a dilatometer at the temperature range of 1200°C-1500°C. During the test, the specimens were quickly heated to the test temperature and held for a period of time (up to 76 hours in this study). The sintering shrinkage was continuously recorded during the test, and the coating shrinkage strains as a function of temperature and time were thus obtained.

EXPERIMENTAL RESULTS

Thermal Conductivity of the TBC/EBC System

Figure 2 shows the thermal conductivity of a 0.58 mm thick ZrO_2–8wt%Y_2O_3/ mullite+BSAS coating system during a 20 hr steady-state testing under the laser high heat flux conditions. The coating had an initial conductivity of 1.7 W/m-K. After the laser thermal exposure at 1482°C surface temperature and 1250°C interface temperature, the average coating conductivity value quickly (in about 3 hrs) increased to 2.35 W/m-K. The conductivity then decreased with the test time. At the end of the 20 hours, the coating conductivity was about 1.9 W/m-K.

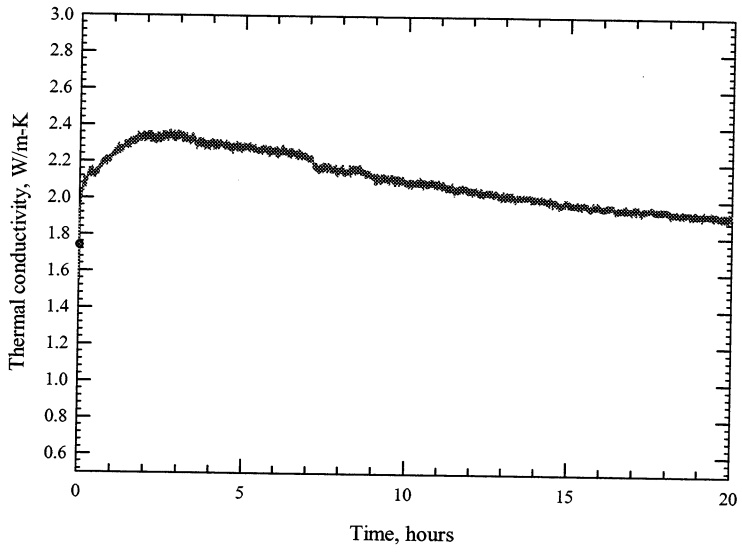

Fig. 2 Thermal conductivity of a 0.58 mm thick ZrO_2–8wt%Y_2O_3/mullite+BSAS coating system during 20 hr laser steady-state testing. The coating surface and interface test temperatures were 1482°C and 1250°C, respectively.

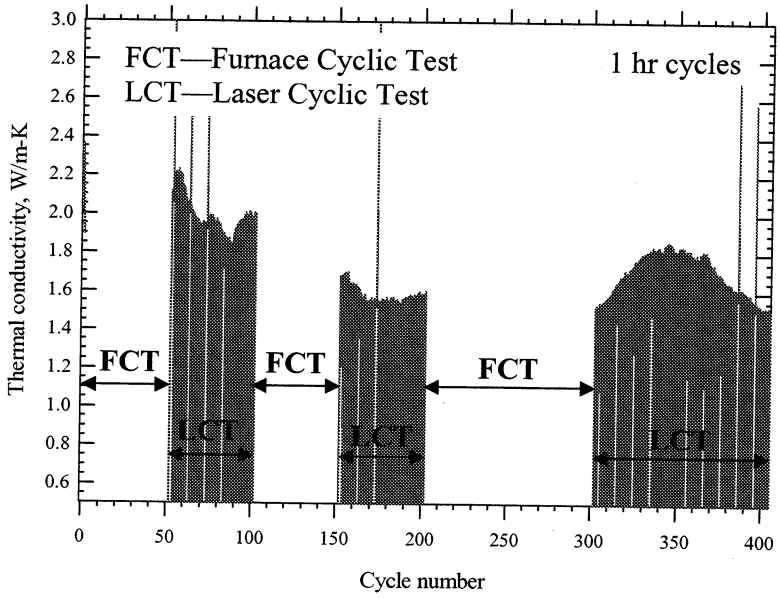

Fig. 3 Thermal conductivity variations of a 0.58 mm thick ZrO_2–8wt%Y_2O_3/mullite+BSAS coating system during the combined laser thermal gradient cyclic test in air (with the coating surface and interface test temperatures at 1482°C and 1250°C) and the furnace thermal cyclic test in 90% water vapor environment at 1300°C. The 60 min hot time cycles were used for both the laser and furnace tests.

This coating specimen was further subjected to a combined testing of furnace thermal cycling in a 90% water vapor environment and laser thermal gradient cycling in air. The coating thermal conductivity was measured *in-situ* during the laser portion of the thermal cyclic test, and the results are shown in Fig. 3. It can be seen that the alternating furnace and laser thermal cyclic tests resulted in significant coating thermal conductivity variations. The coating conductivity changed from the highest value 2.3 W/m-K during the first laser test cycle to about 1.5 W/m-K after 400 cycles of the combined laser and furnace test.

After the first 50 furnace cycle exposure, the coating thermal conductivity increased from 1.9 W/m-K (measured after the first 20 hr laser testing) to 2.1 W/m-K. During the subsequent 50 laser test cycles, the coating conductivity first increased to about 2.2 W/m-K, then generally decreased as the cycle number increased, dropping to about 2.0 W/m-K at the end of the laser test cycles. During the rest of the furnace and laser thermal cycles, the overall coating conductivity showed a general trend to decrease with further thermal cycling. The largest conductivity reduction (~17% reduction) was observed after the second 50 cycle furnace cycles. The thermal conductivity changes after each segment of laser or furnace cycling are illustrated in Fig. 4.

Similar thermal conductivity behavior, i.e., the initial conductivity increase and later conductivity decease, was also observed for the coating system in laser only thermal cyclic tests [16]. Figure 5 summarizes the measured conductivities, after the first 50 cycles and 200 cycles, respectively, for the coating specimens subjected to the combined laser-furnace water vapor test, and the laser only tests at two interface temperatures (1250°C and 1300°C). The effects of the water vapor environment and interface test temperature are clearly demonstrated: the water vapor or high interface test temperature promoted larger initial conductivity increases due to increased coating sintering, but enhanced later conductivity decreases due to accelerated coating delamination.

Figure 6 shows the measured coating conductivity as a function of the cycle frequency. It can be seen that the measured coating conductivity decreases (as debond increases) with the cycle frequency. The conductivity decrease (or the debond increase) with increasing the cycle frequency may suggest the crack healing and cyclic fatigue effect during the laser testing.

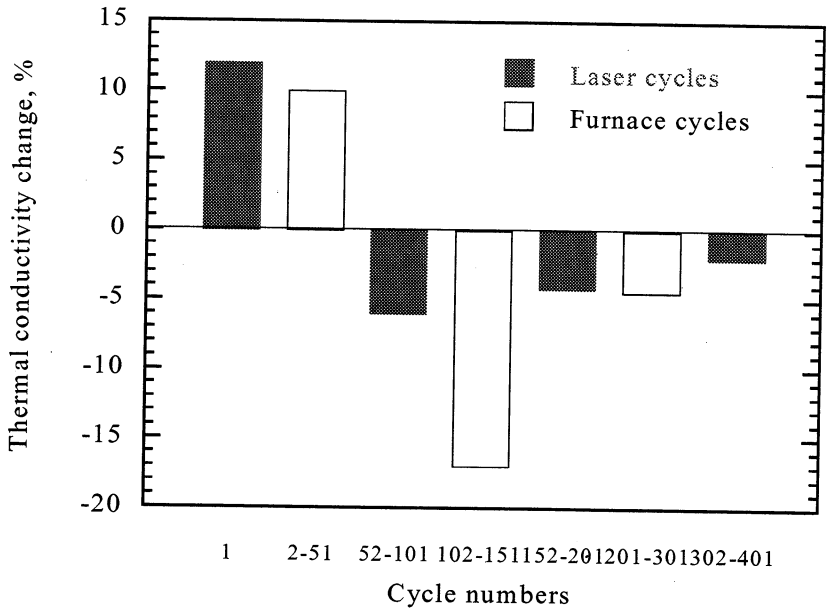

Fig. 4 Thermal conductivity changes during the combined laser and furnace cycles showing conductivity initially increased then decreased with cycle numbers.

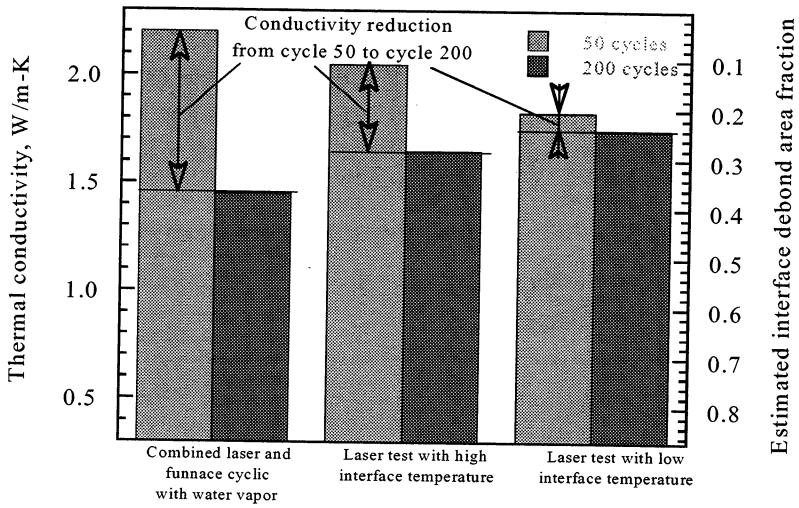

Fig. 5 Thermal conductivity increases and reductions for various laser cyclic tests showing the effects of the water vapor environment and interface test temperature. The presence of water vapor and the higher interface test temperature promotes initial conductivity increases due to coating sintering and interface reaction, but accelerates later conductivity reductions due to the weakened interface and thus more severe coating delaminations.

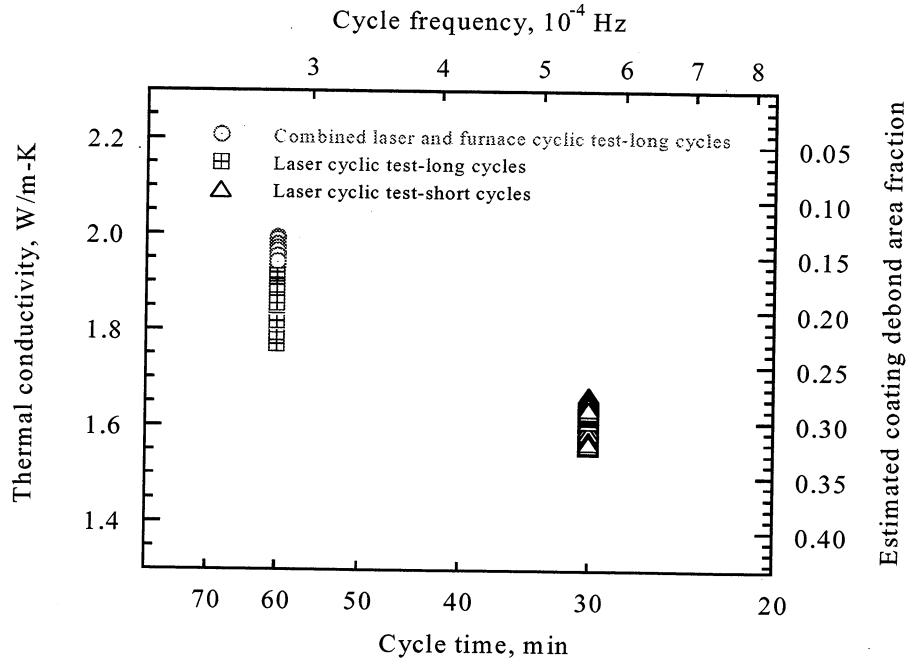

Fig. 6 Measured coating conductivity as a function of the cycle frequency. The coating conductivity decrease (or debond increase) with increasing cycle frequency may suggest the crack healing and cyclic effect during the laser cyclic testing.

Sintering Behavior of ZrO_2–8wt%Y_2O_3 and Mullite Coatings

The sintering shrinkage for ZrO_2–8wt%Y_2O_3 and mullite was shown in Fig. 7. It can be seen that the coating shrinkage strain can be as high as 1% after a 76 hr isothermal testing at 1500°C. The mullite shrinkage strain was found to be 0.3% after ~20 hr testing at 1400°C.

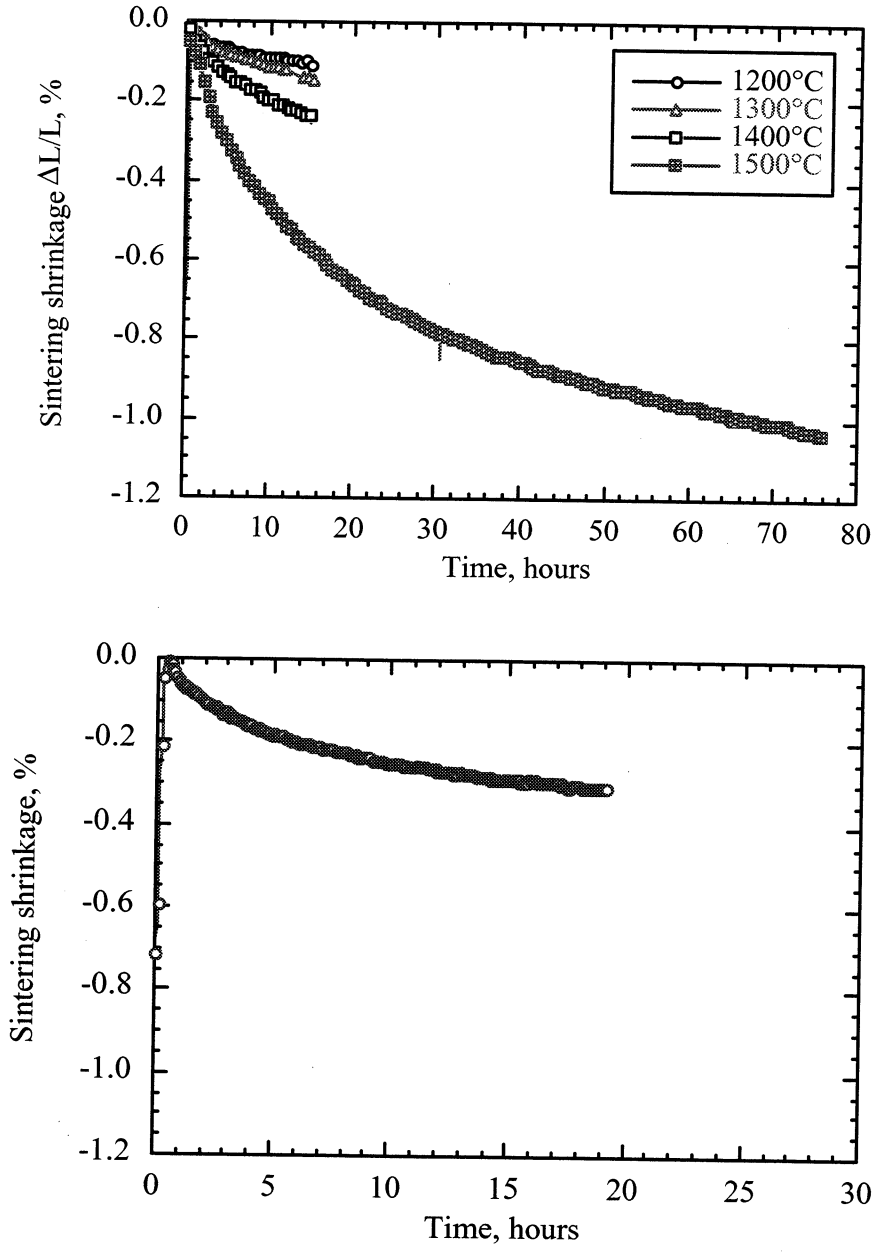

Fig. 7 The sintering-shrinkage strain measured for a plasma-sprayed ZrO_2–8wt%Y_2O_3 coating in a dilatometer thermal expansion test as a function of test time at various temperatures. (a) ZrO_2–8wt%Y_2O_3; (b) mullite.

Failure Modes of the TBC/EBC System

The coating failure modes were investigated during the testing. Figure 8 shows typical coating surface and cross-section cracking morphologies after the laser high thermal gradient test. As shown in Fig. 8 (a), extensive mud-flat cracking was developed on the coating surface after 134 laser cycles (60 min hot time laser cycling). The size of the major surface crack segments typically ranged from 0.5 to 1 mm. The general surface-cracking pattern was observed for all the tested specimens. It should be mentioned that the surface cracking was found to occur even at an early stage of the laser testing (e.g., after the 20 hr laser steady-state 1 cycle test), although the crack widths and crack density usually increased with test cycle. From the cross-section micrographs of the tested coating specimen (Fig. 8 (b)), it can be seen that the surface cracks tended to be wedge-shaped, with the larger crack opening widths near the coating surface and within the ZrO_2–8wt%Y_2O_3 layer. Surface initiated cracks later extended deeply into the mullite and BSAS mixture coatings under the thermal cyclic loading, resulting in severe EBC coating damage and subsequently TBC/EBC coating delaminations and spallations.

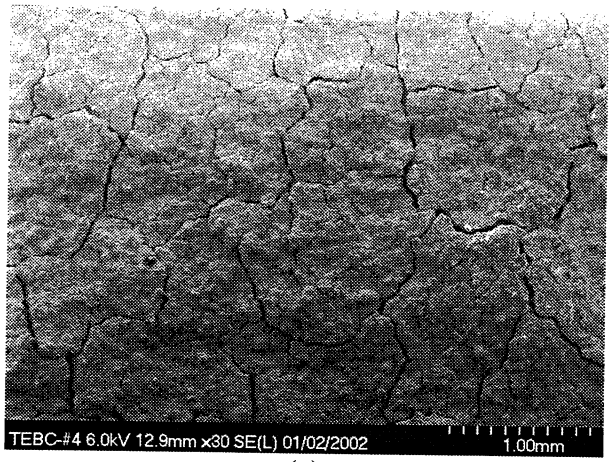

(a)

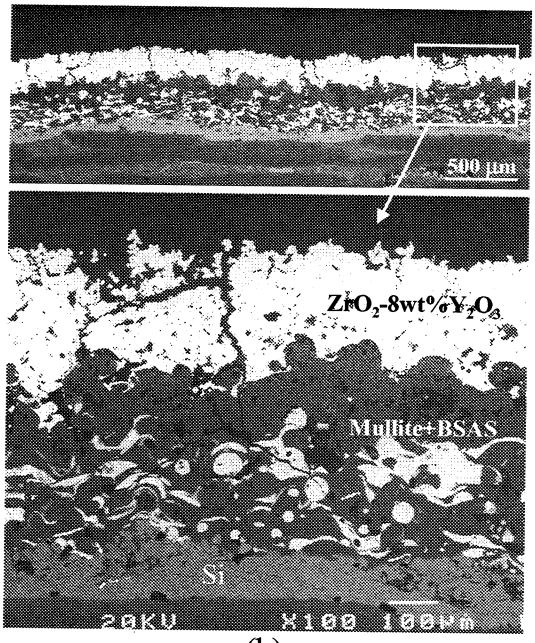

(b)

Fig. 8 Micrographs of typical coating surface and cross-section cracking morphologies of a ZrO_2–8wt%Y_2O_3/mullite+BSAS/Si multi-layered coating system after the laser thermal gradient cyclic testing. (a) The coating surface morphology showing the extensive surface crack networks developed after the laser testing; (b) The coating cross-section micrographs showing the wedge-shape surface cracks and the resulting coating delaminations under the laser thermal gradient cyclic test conditions.

Figure 9 shows cross-section micrographs of a severely delaminated coating specimen, following testing under the combined laser and furnace water vapor cyclic conditions in. It can be seen that the extensive coating cracking occurred in both ZrO_2–8wt%Y_2O_3 and mullite-BSAS coatings. The coating interface, including the Si layer, was also severely damaged from the thermal stresses and the water vapor attack made possible because of the presence of the coating cracks.

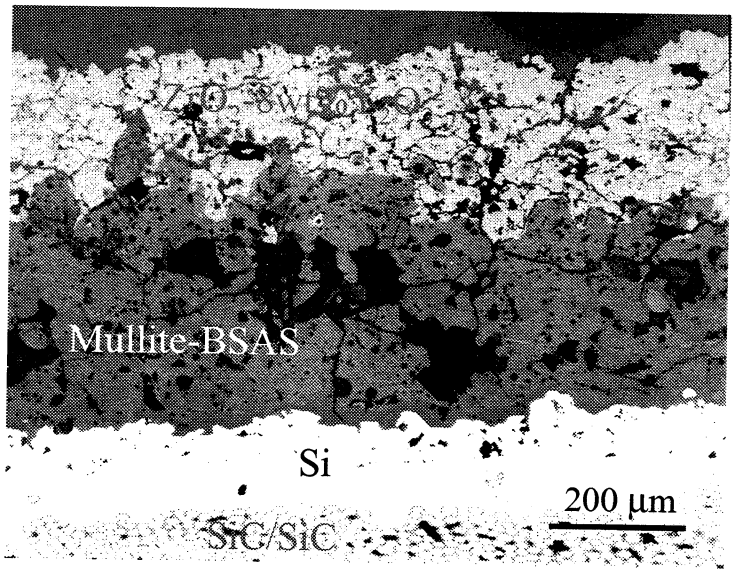

(a)

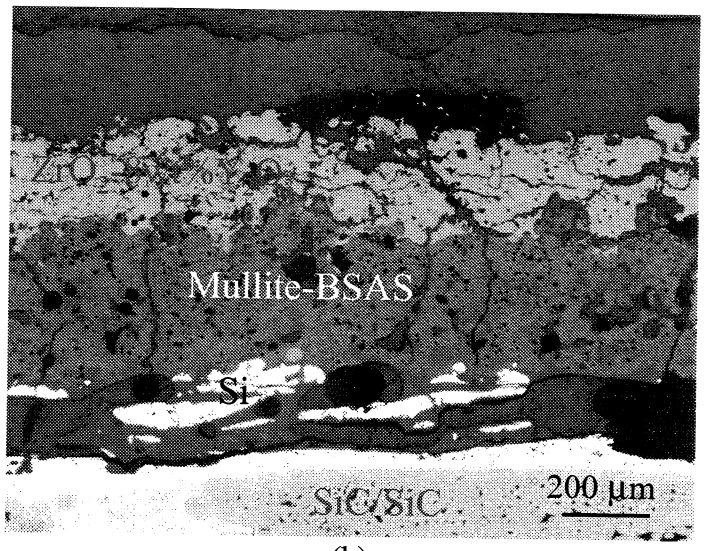

(b)

Fig. 9 Cross-section micrographs, from severely delaminated and interface damaged areas, of a coating specimen tested under the combined laser and furnace water vapor cyclic conditions in. (a) Severely cracked coating region; (b) delaminated coating region.

DISCUSSION

In both the laser and combined laser/furnace tests, the specimen thermal conductivity initially increased due to coating sintering. The coating conductivity increases for individual ZrO_2–8wt%Y_2O_3 thermal barrier and silicate-based environmental barrier coatings have been experimentally demonstrated previously [7, 9, 12, 14].

For the BSAS and mullite/BSAS environmental barrier coatings, it has also been reported that the combined laser cyclic test in air and furnace cyclic test in water vapor environments caused faster coating sintering and a greater conductivity increase at the initial cyclic stage than where tested only in the laser thermal cycling test in air [12]. In the present study, a consistent finding was observed; the combined laser and furnace test resulted in the highest overall conductivity increase in the first 50 cycles for the TBC/EBC system as compared to the laser only tests in air. The enhanced coating sintering under the combined laser and furnace cycle tests may be attributed to the enhanced sintering of the ceramic coatings and the faster silica formation and interface reactions at the interface in the water vapor environments. The laser only test at a higher interface test temperature also enhanced the coating sintering, thus resulting in higher initial conductivity as compared to that with a lower test temperature.

The very fast initial increase in the coating sintering shrinkage strain at the high temperatures, observed from the dilatometer tests, resulted in the formation of surface cracking in relatively short test times. Once the surface cracks are formed, the coating delamination cracks were then initiated and propagated under the cyclic stresses originating from the further sintering-creep shrinkages, and the thermal expansion mismatch between the ZrO_2–8wt%Y_2O_3 top-coat, and the EBC and CMC substrate during the testing. The conductivity variations during the laser tests are attributed to a competing process of the sintering related crack healing, and new crack formation and crack propagation under thermal cycling conditions.

The coating conductivity decrease under the cyclic testing was primarily due to the coating cracking and delaminations. The processes are complex in nature and are closely related to the coating sintering-creep (a time- and temperature-dependent process) and cyclic fatigue (a cycle frequency dependent process, as demonstrated in the cycle frequency effect) under thermal cycling conditions. It should be mentioned that the conductivity decrease was observed even in the first 20 hr steady-state laser testing, indicating possible crack formations and coating delaminations due to the high sintering shrinkage at test temperature before the first cooling cycle. After the laser cyclic test, extensive wedge-shaped surface cracks developed. The wedge–shaped cracks are often generated due to the ceramic coating sintering shrinkage, and the compressive thermal stress-enhanced coating creep within the ZrO_2–8wt%Y_2O_3 at laser test temperatures [6]. Thus, one can correlate the cracking morphologies to the laser thermal gradients within the coating, and predict the surface crack evolution as a function of time [6].

More severe coating delaminations, as indicated by an ultimate lower apparent coating conductivity, were observed for the specimen under the combined furnace water vapor and laser cyclic test conditions, and for the specimen tested under a higher interface temperature with shorter cycle times. It was previously reported that the water vapor had a detrimental effect on EBC coating durability by promoting the coating/substrate interfacial pore formation for the EBC systems under the combined laser and furnace water vapor testing [12]. This behavior leads to faster coating conductivity reductions under the laser thermal cyclic testing. The surface vertical cracks, penetrating into the TBC and EBC, will further accelerate coating degradation.

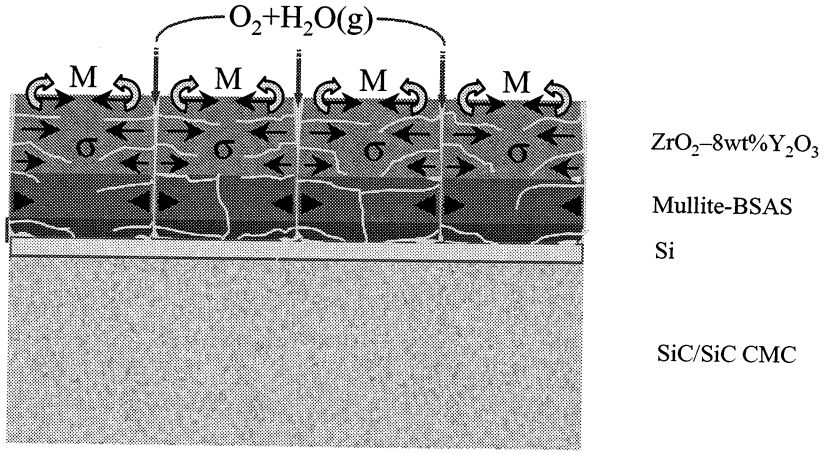

Fig. 10 Coating failure mechanisms of thermal and environmental barrier coating under laser thermal gradient cyclic testing. The surface wedge shape cracks will be generated under the thermal gradient test conditions due to the combined effect of coating sintering and thermal expansion mismatches between the coating layers and the substrate. Upon further cycling the surface cracks will propagate deeply into the EBC and ultimately reach the coating/Si-substrate interface. The water vapor attack further enhances the interface degradation and coating delamination process.

As a result, substantial coating delamination and spallation were observed for the specimen tested under the combined laser and in the furnace water vapor environments. The laser test at a higher interface temperature will also result in more coating interface damage and weak interface bonding during the later stage of testing, leading to more conductivity reductions than laser tests at a lower interface temperature. The accelerated damage, with increasing cycle frequency, under more frequent cycle test (30 min cycle test) also suggests a possible cyclic fatigue effect in addition to the time dependent sintering-creep effect for the TBC/EBC coating systems. The coating failure mechanism is summarized in Fig 10.

CONCLUSIONS

A laser heat flux test approach has been used to investigate thermal cyclic behavior and conductivity response of plasma-sprayed ZrO_2–8wt%Y_2O_3/mullite+BSAS/Si coating systems. The conductivity variations can be attributed to a competing process of coating sintering and coating delamination cracking. The coating failure involved both the time-temperature dependent sintering and the cycle frequency dependent cyclic fatigue processes. Water vapor environments promoted initial conductivity increases, due to enhanced coating sintering and interface reaction, and later conductivity reductions due to accelerated coating cracking and delaminations. The failure of the coating system can be characterized as wedge-shape surface cracking, and surface cracking-enhanced coating delamination.

REFERENCES

[1] K.N. Lee and R.A. Miller, "Development and Environmental Durability of Mullite and Mullite/YSZ Dual Layer Coatings for SiC and Si3N4 Ceramics," *Surface and Coatings Technology*, vol. 86–87, pp. 142–148, 1996.

[2] K.N. Lee, "Key Durability Issues with Mullite-Based Environmental Barrier Coatings for Si-Base Ceramics," *Transactions of the ASME*, vol. 122, pp. 632–636, 2000.

[3] K.N. Lee, "Current Status of Environmental Barrier Coatings for Si-Based Ceramics," *Surface and Coatings Technology*, vol. 133–134, pp. 1–7, 2000.

[4] D. Zhu, K.N. Lee, and R.A. Miller, "Thermal Conductivity and Thermal Gradient Cyclic Behavior of Refractory Silicate Coatings on SiC/SiC Ceramic Matrix Composites," NASA Glenn Research Center, Cleveland, Ohio, NASA TM–210824, April 2001.

[5] D. Zhu and R.A. Miller, "Investigation of Thermal High Cycle and Low Cycle Fatigue Mechanisms of Thick Thermal Barrier Coatings," *Materials Science and Engineering*, vol. A245, pp. 212–223, 1998.

[6] D. Zhu and R.A. Miller, "Determination of Creep Behavior of Thermal Barrier Coatings under Laser Imposed High Thermal and Stress Gradient Conditions," *Journal of Materials Research*, vol. 14, pp. 146–161, 1999.

[7] D. Zhu and R.A. Miller, "Thermal Barrier Coatings for Advanced Gas-Turbine Engines," *MRS Bulletin*, vol. 27, pp. 43–47, 2000.

[8] D. Zhu and R.A. Miller, "Thermophysical and Thermomechanical Properties of Thermal Barrier Coating Systems," NASA Glenn Research Center, Cleveland, NASA TM–210237, July 2000.

[9] D. Zhu and R.A. Miller, "Thermal Conductivity and Elastic Modulus Evolution of Thermal Barrier Coatings Under High Heat Flux Conditions," *Journal of Thermal Spray Technology*, vol. 9, pp. 175–180, 2000.

[10] D. Zhu, R.A. Miller, B.A. Nagaraj, and R.W. Bruce, "Thermal Conductivity of EB-PVD Thermal Barrier Coatings Evaluated by a Steady-State Laser Heat Flux Technique," *Surface and Coatings Technology*, vol. 138, pp. 1–8, 2001.

[11] D. Zhu, S.R. Choi, and R.A. Miller, "Thermal Fatigue and Fracture Behavior of Ceramic Thermal Barrier Coatings," *Ceramic Engineering and Science Proceedings*, vol. 22, pp. 453–461, 2001.

[12] D. Zhu, K.N. Lee, and R.A. Miller, "Thermal Conductivity and Thermal Gradient Cyclic Behavior of Refractory Silicate Coatings on SiC/SiC Ceramic Matrix Composites," *Ceram. Eng. Sci. Proc.*, vol. 22, pp. 443–452, 2001.

[13] D. Zhu and R.A. Miller, "Thermal Conductivity and Elastic Modulus Evolution of Thermal Barrier Coatings Under High Heat Flux Conditions," NASA Glenn Research Center, Cleveland, Ohio, NASA TM–209069, April 1999.

[14] D. Zhu, N.P. Bansal, K.N. Lee, and R.A. Miller, "Thermal Conductivity of Ceramic Thermal Barrier and Environmental Barrier Coating Materials," NASA Glenn Research Center, Cleveland NASA TM–211122, September 2001.

[15] D. Zhu and R.A. Miller, "Thermophysical and Thermomechanical Properties of Thermal Barrier Coating Systems," *Ceram. Eng. Sci. Proc.*, vol. 21, pp. 623–633, 2000.

[16] D. Zhu, K.N. Lee, and R.A. Miller, "Thermal Gradient Cyclic Behavior of Thermal and Environmental Barrier Coating Systems on SiC/SiC Ceramic Matrix Composites," presented at ASME TURBO EXPO 2002, Amsterdam, The Netherlands, 2002.

REPORT DOCUMENTATION PAGE

Form Approved
OMB No. 0704-0188

1. AGENCY USE ONLY (*Leave blank*)	2. REPORT DATE	3. REPORT TYPE AND DATES COVERED
	April 2002	Technical Memorandum

4. TITLE AND SUBTITLE

Cyclic Failure Mechanisms of Thermal and Environmental Barrier Coating Systems Under Thermal Gradient Test Conditions

5. FUNDING NUMBERS

WU–714–04–20–00

6. AUTHOR(S)

Dongming Zhu, Kang N. Lee, and Robert A. Miller

7. PERFORMING ORGANIZATION NAME(S) AND ADDRESS(ES)

National Aeronautics and Space Administration
John H. Glenn Research Center at Lewis Field
Cleveland, Ohio 44135–3191

8. PERFORMING ORGANIZATION REPORT NUMBER

E–13245

9. SPONSORING/MONITORING AGENCY NAME(S) AND ADDRESS(ES)

National Aeronautics and Space Administration
Washington, DC 20546–0001

10. SPONSORING/MONITORING AGENCY REPORT NUMBER

NASA TM—2002-211478

11. SUPPLEMENTARY NOTES

Prepared for the 26th Annual International Conference on Advanced Ceramics and Composites sponsored by the American Ceramics Society, Cocoa Beach, Florida, January 13–18, 2002. Dongming Zhu, Ohio Aerospace Institute, 22800 Cedar Point Road, Brook Park, Ohio 44142; Kang N. Lee, Cleveland State University, Cleveland, Ohio 44115; and Robert A. Miller, NASA Glenn Research Center. Responsible person, Dongming Zhu, organization code 5160, 216–433–5422.

12a. DISTRIBUTION/AVAILABILITY STATEMENT

Unclassified - Unlimited
Subject Categories: 24 and 27 Distribution: Nonstandard

Available electronically at http://gltrs.grc.nasa.gov/GLTRS

This publication is available from the NASA Center for AeroSpace Information, 301–621–0390.

12b. DISTRIBUTION CODE

13. ABSTRACT ***(Maximum 200 words)***

Plasma-sprayed ZrO_2–8wt%Y_2O_3 and mullite+BSAS/Si multilayer thermal and environmental barrier coating (TBC-EBC) systems on SiC/SiC ceramic matrix composite (CMC) substrates were thermally cyclic tested under high thermal gradients using a laser high-heat-flux rig in conjunction with furnace exposure in water-vapor environments. Coating sintering and interface damage were assessed by monitoring the real-time thermal conductivity changes during the laser heat-flux tests and by examining the microstructural changes after exposure. Sintering kinetics of the coating systems were also independently characterized using a dilatometer. It was found that the coating failure involved both the time-temperature dependent sintering and the cycle frequency dependent cyclic fatigue processes. The water vapor environments not only facilitated the initial coating conductivity increases due to enhanced sintering and interface reaction, but also promoted later conductivity reductions due to the accelerated coating cracking and delamination. The failure mechanisms of the coating systems are also discussed based on the cyclic test results and are correlated to the sintering and thermal stress behavior under the thermal gradient test conditions.

14. SUBJECT TERMS

Thermal barrier coatings; Environmental barrier coatings; Thermal gradient; Cyclic testing; Thermal conductivity; Failure mechanisms

15. NUMBER OF PAGES

19

16. PRICE CODE

17. SECURITY CLASSIFICATION OF REPORT	18. SECURITY CLASSIFICATION OF THIS PAGE	19. SECURITY CLASSIFICATION OF ABSTRACT	20. LIMITATION OF ABSTRACT
Unclassified	Unclassified	Unclassified	